Available online at www.sciencedirect.com
ScienceDirect
Journal of Solid State Chemistry 180 (2007) 510–517
JOURNAL OF SOLID STATE CHEMISTRY
www.elsevier.com/locate/jssc

High-pressure phase transition in $LiBH_4$

A.V. Talyzin[a,*], O. Andersson[a], B. Sundqvist[a], A. Kurnosov[b], L. Dubrovinsky[b]

[a]*Department of Physics, Umeå University, S-90187 Umeå, Sweden*
[b]*Bayerisches Geoinstitut, Universität Bayreuth, D-95440 Bayreuth, Germany*

Received 18 August 2006; received in revised form 27 October 2006; accepted 29 October 2006
Available online 10 November 2006

Abstract

The high-pressure phase transition from ambient pressure α-$LiBH_4$ to high-pressure β-$LiBH_4$ was observed by Raman spectroscopy and X-ray diffraction between 0.8 and 1.1 GPa. The phase boundary between these two phases was mapped over a large range of temperatures using thermal conductivity studies and differential thermal analysis. The structure of the high-pressure phase could not be identified due to small number of experimentally observed reflections, but it was shown that it is different from previously reported theoretical predictions.

Keywords: High pressure; Borohydrides; Phase transition; Raman spectroscopy

1. Introduction

Complex hydrides (alanates and borohydrides) have attracted considerable attention recently due to their possible application as hydrogen storage materials. High-pressure studies for some of these materials were performed already about half-century ago but in spite of this only limited information is yet available. Much of the recent activities in high-pressure studies of these materials was stimulated by theoretical studies performed by Vajeeston et al. who predicted a large volume collapse for high-pressure modifications of $LiAlH_4$ and $NaAlH_4$ [1,2]. Experimental studies showed that phase transitions do occur in these materials at high-pressure conditions, though not exactly into the predicted structures [3,4]. Similar studies have recently been initiated also on borohydrides. Two high-pressure phase transitions were observed experimentally for $NaBH_4$ using diamond anvil cell (DAC) methods and thermal conductivity measurements [5–7].

The ambient phase of $LiBH_4$ was recently studied in detail due to the interest in the hydrogen storage properties of this material. Both the Raman spectrum and the crystal structure of this phase are well known. At room temperature and normal pressure $LiBH_4$ crystallizes in an orthorhombic structure (space group *Pnma*, $a = 7.17858(4)$, $b = 4.43686(2)$, $c = 6.80321(4)$) Å [8]. It is usually described to be composed of tetrahedral $(BH4)^-$ anions and Li^+ cations. A structural transition was reported to occur in this phase upon heating, at ~381 K [9–11]. According to more recent data this phase transition involves also some minor loss of hydrogen and the exact nature of this transition is not clear at the moment [12]. Borohydrides with *fcc* lattice-related structure ($NaBH_4$, KBH_4, $RbBH_4$, $CsBH_4$) are known to undergo phase transitions into more ordered phases at low temperatures and ambient pressure [13,14]. However, the crystal structure of $LiBH_4$ is different from that of the above compounds and no phase transition has been observed at low temperatures at atmospheric pressure [15]. On the other hand, a very careful study of phase transformations in $LiBH_4$ at high pressure, at and above room temperature, was carried out by Pistorius [11] about 40 years ago. Until now, this remains the only available experimental study in this field. A phase transition into an almost 6% denser high-pressure phase was observed in Pistorius' volume measurements to occur at around 0.6 GPa at 298 K and 0.84 GPa at 341 K [11], but the transition was associated with a quite large hysteresis. This new phase was stable to the highest pressure investigated, 4.5 GPa. Two additional high-pressure phases

*Corresponding author. Fax: +46 90 786 66 73.
E-mail address: ppsh1@mail.ru (A.V. Talyzin).

0022-4596/$ - see front matter © 2006 Elsevier Inc. All rights reserved.
doi:10.1016/j.jssc.2006.10.032

were observed above 370 K, but since structural data were not collected in this study the natures of these three high-pressure phases are unknown. Recently, the structural stability of $LiBH_4$ was studied theoretically by several groups. Łodziana et al. [16] predicted a phase transition into a monoclinic high-pressure phase with space group Cc to occur at ~3 GPa. Another theoretical prediction was recently given by Vajeeston et al. [17]. In this study, a phase transition into the tetragonal β-KBH_4 type of structure was proposed to occur at 6.2 GPa. The high-temperature hexagonal phase of $LiBH_4$ was predicted to be stable at pressures below 6.2 GPa and assumed to be the high-pressure phase found by Pistorius [11]. A third study by Frankcombe et al. [18] suggests that $LiBH_4$ should transform first into a $P2_1/c$ phase at 1 GPa, then into the Cc structure near 2.2 GPa.

We present the results of a set of experiments performed using the DAC. Raman spectra and XRD patterns were collected at pressures up to ~9 GPa at room temperature. We have also used thermal conductivity measurements and differential thermal analysis (DTA) as a tool to map for the first time the phase transition boundary between the ambient pressure α-$LiBH_4$ and high-pressure β-$LiBH_4$ phases to below 200 K. We show that this transition has a very large hysteresis and present the high-pressure phase diagram of $LiBH_4$ below 370 K.

2. Experimental details

$LiBH_4$ of 99.9% purity was purchased from Sigma–Aldrich and used without additional purification. Raman spectra and XRD data recorded on the purchased powder showed only $LiBH_4$ without any peaks from impurity phases. High-pressure experiments were performed using a DAC with 0.4 mm flat culets. The sample was loaded into a 0.2 mm hole in the steel gasket together with a ruby chip used for pressure calibration. In the XRD experiments, a small piece of gold wire was added for calibration. No pressure medium was used. The initial thickness of the sample was 60–70 μm. Since the material is sensitive to moisture, the loading was performed in a glovebox under argon gas. Raman spectra of the starting material and for the sample loaded into the DAC were identical, which confirmed that the loading procedure had not affected the sample. The pressure was increased gradually in steps of 1–1.5 GPa, and Raman spectra were recorded at every step during compression and decompression. Usually, the time of treatment at each pressure step was about 1–2 h. A Renishaw 1000 Raman spectrometer with a 633 nm excitation laser and a resolution of 2 cm^{-1} was used in these experiments. Raman spectra were recorded in situ through the diamond anvils using long focus ×20–50 objectives.

The XRD data were recorded with a system consisting of Rigaku FRD high-brilliance generator (90 kW) and an APEX CCD Area Detector. The Mo$K\alpha$ radiation (tube voltage 60 kV, tube current 55 mA, cathode gun $0.1 \times 0.1\ mm^2$) was focused with MaxFlux X-ray optics and further collimated down to 40 μm FWHM beam size. The two-dimensional XRD patterns were integrated using Fit2D software.

As in a previous experiment [7], the thermal conductivity κ was measured using the hot wire method [19] with a 0.1 mm in diameter Ni wire probe. In the present experiment, half of the cylindrical pressure cell was filled with solid Teflon® and the remaining semi-circular segment filled with $LiBH_4$ powder, packed as dense as possible. The Ni wire probe was arranged inside the specimen at a constant distance from the periphery to minimize pressure gradients, since there is always a small radial flow of material on compression. The pressure in the cell was determined from load/area with an empirical correction for friction, established in a separate experiment using the pressure dependence of the resistance of a Manganin wire. To enable detection of phase transitions also by DTA, one type K thermocouple was placed in the sample and another one in the bottom of the Teflon® capsule. The sign and magnitude of the output voltage difference between these two thermocouples was monitored continuously. The pressure cell was filled in a glove-box under dry argon gas. The thermal conductivity and DTA experiments were carried out in an all-steel piston-and-cylinder device, 45 mm in inside diameter. The cylinder was fitted with an electrical heater and insulated by fibreglass insulation, and could be cooled by direct spraying with liquid nitrogen. A simple on/off regulator could keep the pressure cylinder at a reasonably constant temperature both above and below room temperature. The large thermal mass of the cylinder ensured good short-time temperature stability.

3. Results and discussion

3.1. Raman study in DAC

The Raman spectrum of $LiBH_4$ at ambient conditions is well known [20,21]. The high-frequency region exhibits several peaks due to internal $B-H$ vibrations and some combinational modes. In our spectra, the major peaks are found at 2320, 2300, 2275, 2181, and 2161. The intermediate-frequency region shows four peaks due to bending modes in the range from 1000 to 1400 cm^{-1}. Finally, the low-frequency region below 600 cm^{-1} exhibits librational and translational modes. These peaks were too weak to be observed in our high-pressure experiments. The spectrum recorded from the pristine material was in good agreement with literature data [20].

Raman spectra of $LiBH_4$ recorded while increasing the pressure are shown in Fig. 1. Comparing spectra recorded at 0.5–1.4 GPa, clear changes are visible. These changes are interpreted in terms of a phase transition from ambient pressure α-$LiBH_4$ to a high-pressure β-$LiBH_4$ phase, in good agreement with the previous study by Pistorius [11] who observed a transition at ~0.7 GPa at room

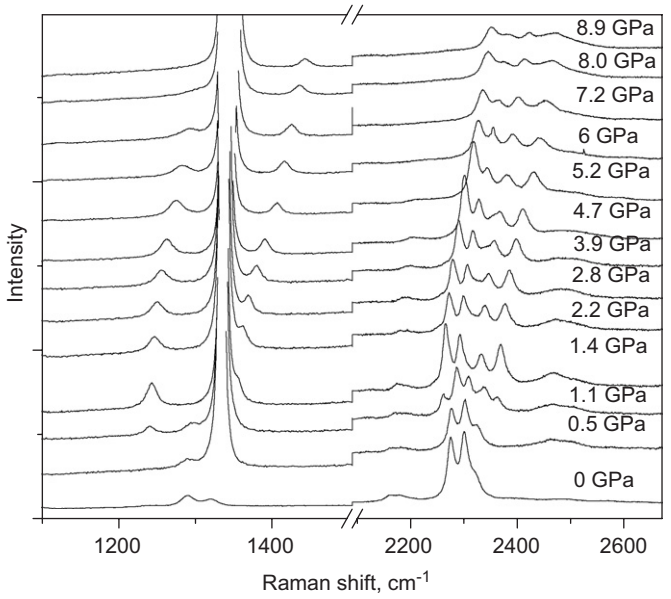

Fig. 1. Raman spectra recorded during compression of $LiBH_4$.

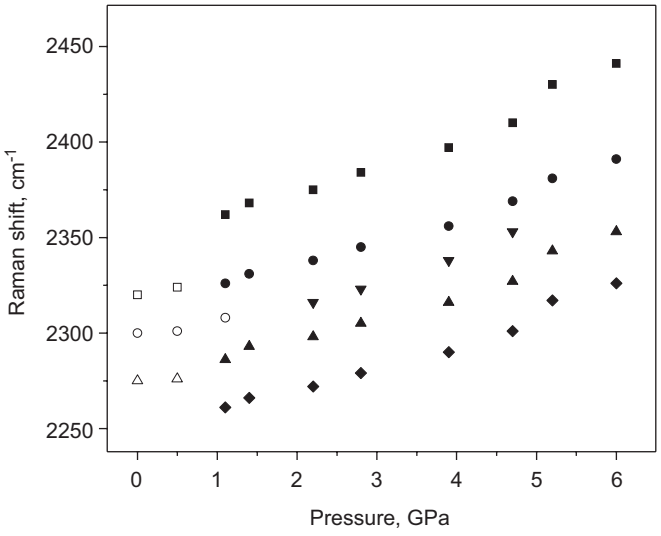

Fig. 2. Pressure dependence of peak positions for the strongest $LiBH_4$ modes. Open symbols mark peaks from the ambient pressure phase and filled symbols for the high-pressure phase.

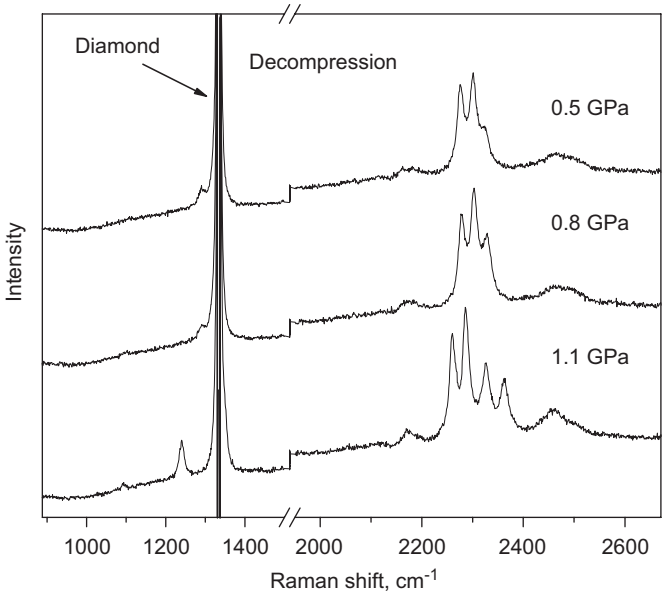

Fig. 3. Raman spectra in the region of the phase transition recorded during decompression.

temperature. The spectrum recorded at 1.1 GPa clearly shows co-existence of both ambient and high-pressure phases, while at 1.4 GPa the phase transformation is complete. The high-pressure phase is characterized by four strong peaks and two weaker peaks in the high wavenumber region above 2000 cm^{-1} and at least two peaks in the region of bending modes. The observation of bending modes is complicated by the broad peak from the diamond anvils which overlaps with $LiBH_4$ modes in some spectra. The pressure dependencies of some peak positions are shown in Fig. 2.

Above 6 GPa we observe a broadening of some peaks and a change in their relative intensities, but the main spectral features remain unchanged and the β-$LiBH_4$ phase seems to remain stable up to 8.9 GPa. The phase transition observed during the compression run appeared to be completely reversible upon pressure decrease (see Fig. 3). The spectrum recorded at 0.8 GPa still shows some weak peaks from the high-pressure phase, but at 0.5 GPa the ambient pressure α-$LiBH_4$ is recovered completely.

It is interesting to discuss how the experimentally observed Raman spectra correspond to theoretically predicted structures. The work by Łodziana et al. [16] suggests a phase transition to a monoclinic phase at around 3 GPa. As can be observed from the Raman spectra, the phase transition occurs at a lower pressure than predicted [16] and it is unlikely that it corresponds to a symmetry decrease. Actually, the number of observed peaks even decreased for the bending modes. Only two peaks due to bending modes were observed in the high-pressure phase compared to four at ambient pressure and the five modes which should be observed for the $P2_1/c$ space group [16]. It can be, however, that some modes were too weak to be observed in the DAC. Vajeeston et al. [17] suggested a new phase above 6.2 GPa with the same tetragonal structure as β-KBH_4. The predicted phase transition pressure is too high compared to our experimental results, but the Raman spectra of β-$LiBH_4$ found in our experiments do show some similarity to the Raman spectrum of KBH_4, as shown in Fig. 4.

The Raman spectrum of β-KBH_4 is not available in the literature but the spectrum for α-KBH_4 can be used instead. The transition from fcc α-KBH_4 phase to β-KBH_4 occurs at low temperature and leaves the shape of BH_4 units unchanged while some rotational freedom freezes. Therefore, for the stretching and bending modes of α-KBH_4 and β-KBH_4 some strong similarity should be

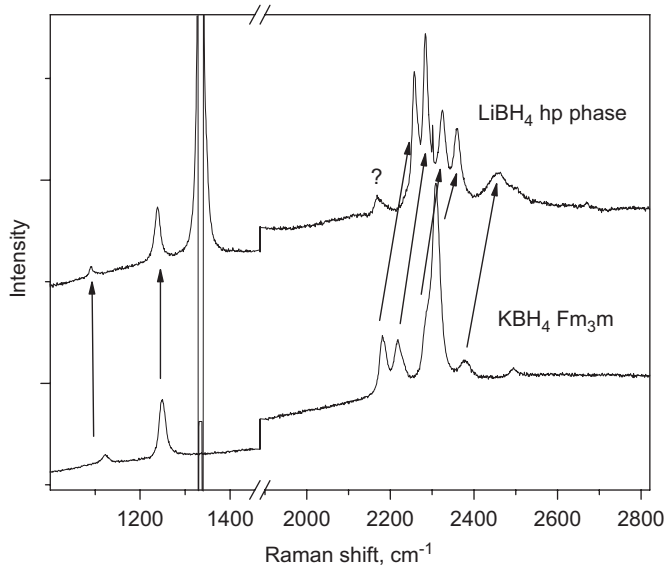

Fig. 4. Raman spectrum of the high-pressure modification of $LiBH_4$ compared to the Raman spectrum of KBH_4 at ambient conditions.

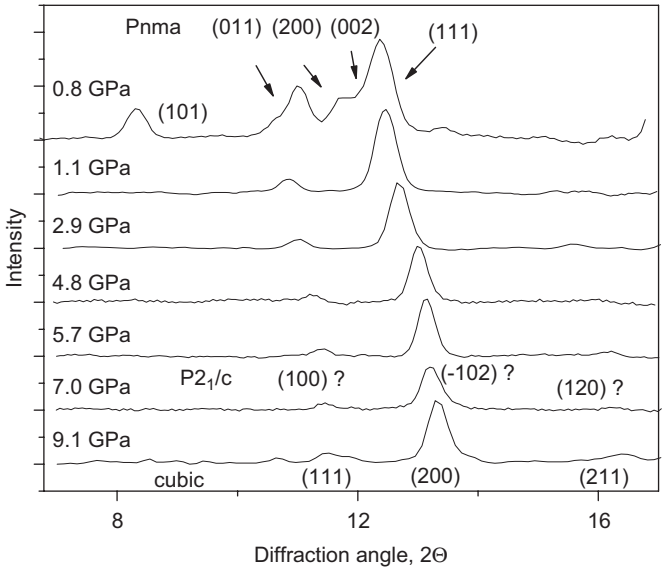

Fig. 5. XRD patterns obtained during compression run from 0.8 to 9.1 GPa.

expected. Such a similarity was, in fact, experimentally observed for the similar phase transition of $NaBH_4$ at low temperatures [5]. Fig. 4 shows some similarity between the Raman spectra of the high-pressure phase of $LiBH_4$ and the ambient pressure phase of KBH_4, but the similarity is not complete as pointed out by the question mark in Fig. 4. The results might be interpreted suggesting that orthorhombic α-$LiBH_4$ shows a phase transition at high pressure into a structure somewhat similar to the low temperature phases of other borohydrides ($NaBH_4$, KBH_4, etc.).

3.2. X-ray diffraction study in DAC

The XRD study was performed in a separate experiment which started at 5 GPa with stepwise decompression until the phase transition from the high-pressure phase to the ambient pressure phase of $LiBH_4$ was completed. After that, XRD patterns were recorded while pressure was increased up to 9 GPa. The high-pressure β-$LiBH_4$ phase persisted down to 1.2 GPa and the phase transition was observed between 1.2 and 0.8 GPa. The XRD pattern recorded at 0.8 GPa can be confidently identified as that of the ambient pressure *Pnma* phase of $LiBH_4$. The pressure was then increased in a new run from 0.8 to 9.1 GPa, during which the high-pressure phase re-appeared above 1 GPa as expected (see Fig. 5). The pressure dependence of the *d*-spacings for the high-pressure phase of $LiBH_4$ up to 9.1 GPa are shown in Fig. 6. The ratio between the largest and smallest *d*-spacings remains almost the same upon compression (in the range 1.41–1.42).

Unfortunately, the pattern for the high-pressure phase exhibits an insufficient number of reflections for structural identification. Only three peaks were observed for the high-pressure phase. It should be taken into account that $LiBH_4$ consists of some of the lightest elements in the periodic

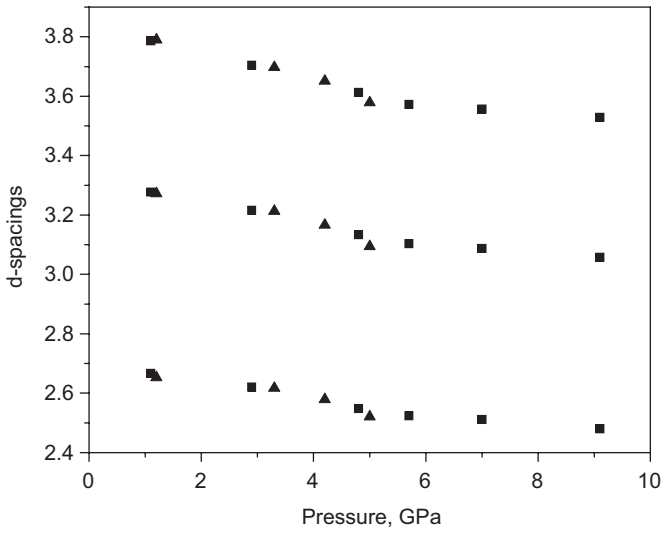

Fig. 6. Pressure dependence of *d*-spacing for the high-pressure β-$LiBH_4$ phase recorded during decompression (triangles) and compression (squares).

table and X-ray scattering from this material is relatively weak. Using conventional (non-synchrotron) radiation it is difficult to expect better results for this material. Nevertheless, even having only three reflections it is possible to compare the data with theoretical predictions and to draw some preliminary conclusions about the structure of the high-pressure phase. Łodziana et al. [16] predicted a phase transition at ~3 GPa into a high-pressure phase with monoclinic structure, space group Cc. Important information can also be found in the early work of Pistorius [11] who reported the phase transition to occur at around 0.7 GPa with a volume collapse of ~5.6%. Comparing our

XRD data to the simulated pattern for the Cc phase predicted by Łodziana et al. [16] shows that this structure with cell parameters similar to those used in Ref. [16] cannot explain the experimentally observed XRD pattern. Therefore, we compared the experimental data with other structures considered by Łodziana et al. [16] in their theoretical study. One of these structures, monoclinic $P2_1/c$ ($a = 7.267$, $b = 7.174$, $c = 7.683$ Å, $\beta = 148.52^\circ$ in Ref. [16]), also suggested by Frankcombe et al. [18], could be fitted to our experimental data using cell parameters very similar to those theoretically predicted. For example, the XRD pattern recorded in our compression run at 1.1 GPa could be fitted reasonably well using the following cell parameters: $a = 7.32$, $b = 7.14$, and $c = 7.75$ Å with $\beta = 148.86^\circ$. The unit cell volume for this suggested high-pressure phase was compared to the unit cell volume calculated for α-$LiBH_4$ at 0.8 GPa which resulted in a difference of only ~0.7%. This value is not in good agreement with the experimentally determined volume change of ~5.6 % found by Pistorius [11].

It can be concluded from our XRD data that available theoretical predictions for the structure of the high-pressure phase of $LiBH_4$ are not confirmed. In principle, the Cc structure is not completely ruled out in our XRD experiments due to the low number of peaks observed, but fitting the observed peaks to this structure would require using cell parameters rather different from those used in the simulations by Lodziana et al. [16]. Better quality XRD can be obtained only using synchrotron radiation.

Before closing this section, we note that the XRD data obtained in the low pressure region (points at ambient pressure and 0.8 GPa) can be used to obtain a very approximate value of $B(0) = 45$ GPa for the bulk modulus of α-$LiBH_4$. This value is a factor of 2–3 higher than the corresponding value for $NaBH_4$ [7], probably reflecting stronger interatomic bonding in the present material.

3.3. Thermal conductivity

While Pistorius [11] mapped the phase diagram of $LiBH_4$ in detail above 370 K, he showed only two experimental points on the phase boundary between α-$LiBH_4$ and β-$LiBH_4$. This transition was also associated with a very large hysteresis of several hundred MPa. We have therefore mapped this phase transition line to lower temperatures using measurements of the thermal conductivity, κ. Such measurements were carried out only at room temperature and below.

In the first run, pressure was first increased to 0.1 GPa to compact the sample and to create good thermal contact between the sample material and the hot wire probe. A first isobaric cooling/heating run was then carried out at this pressure between 290 and 110 K, with the results shown in Fig. 7. After returning to room temperature, pressure was slowly increased to 0.5 GPa, where a second isobaric cooling/heating run was carried out down to 95 K. It is evident from Fig. 7 that no phase transition was observed

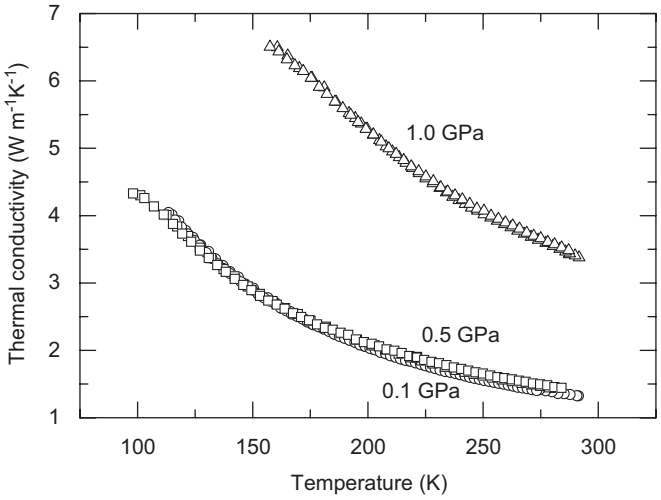

Fig. 7. Thermal conductivity plotted against temperature at three different temperatures.

in either of these runs. Moreover, the data for κ at 0.1 and 0.5 GPa are almost indistinguishable, which is surprising. Normally, κ increases significantly with increasing pressure for crystalline phases, but in this case the pressure dependence is unusually weak with $d\ln\kappa/dp = 0.13\,GPa^{-1}$. The density dependence of κ is described in terms of the Bridgman parameter $g = B \times (d\ln\kappa/dp)_T$ where ρ is the density and B the bulk modulus. Typically, the density dependence of for ordered crystals is larger than about 5, whereas liquids, glasses and other disordered phases have g close to 3. Using the very approximate value $B = 45$ GPa derived above we find $g = 5.85$ near room temperature, which is low but within the range normally found for crystalline materials. The measurements indicate that $d\ln\kappa/dp$ decreases with decreasing temperature, and below 150 K it appears to become negative as shown in Fig. 7. We have not been able to determine whether this interesting effect is real or an experimental artifact only.

The pressure was then increased further, and as shown in Fig. 8a a clear, sharp phase transformation, associated with a very large increase in κ, was observed between 0.7 and 0.8 GPa, in good agreement with XRD and Raman data. The temperature dependence of κ in the high-pressure phase was then investigated by a third isobaric cooling/heating cycle (Fig. 7); the temperature range was limited at the low end to about 155 K where the very high value of κ started to reduce the experimental accuracy. After completion of this cycle the pressure was slowly decreased to 0.2 GPa at room temperature. A very clear reverse transformation to the ambient pressure phase was observed between 0.5 and 0.4 GPa, as shown in Fig. 8a. We note that the observed hysteresis is very large, in agreement with the behaviour observed by Pistorius [11]. However, at least a small part of the indicated difference between the transition pressures on increasing and decreasing pressure is due to the reversal of the friction between the piston and the

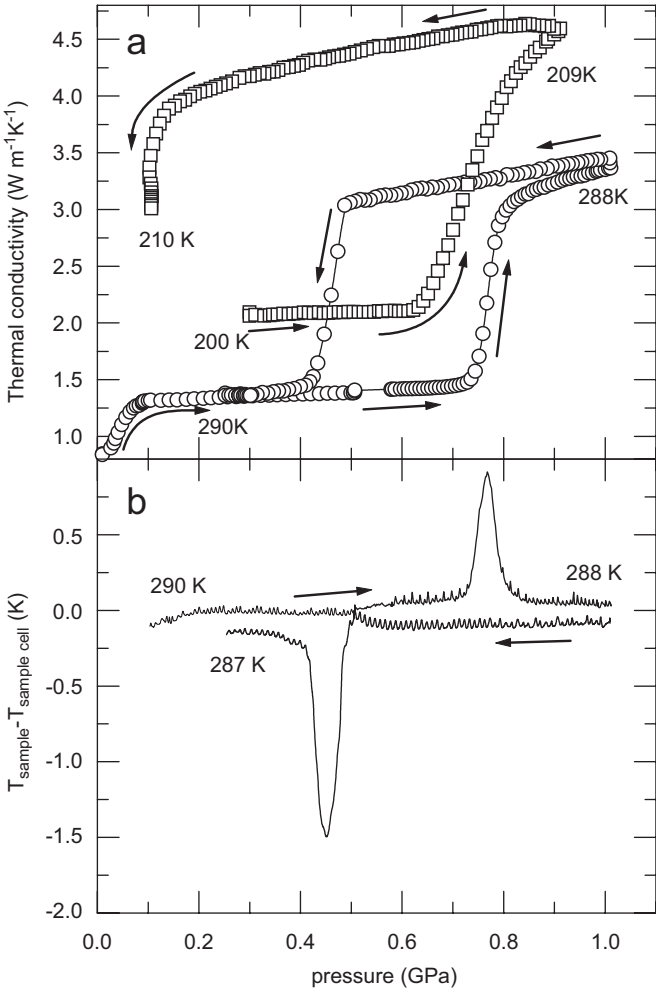

Fig. 8. (a) Thermal conductivity plotted against pressure at 290 and 200 K (b). The temperature difference between sample and cell plotted against pressure at 290 K, measured simultaneously with the data in (a).

cylinder. (The calibration of the pressure was done on increasing pressure).

Since no transition was observed during the isobaric temperature runs we decided to make a second isothermal pressure run at low temperature to define the transition line better. We thus cooled the cell to about 200 K at 0.3 GPa, during which run we obtained data for κ of the same magnitude as those found at 0.1 and 0.5 GPa. The pressure was then cycled from 0.3 up to 0.9 GPa and back down to 0.1 GPa, as shown in Fig. 8. Again, a very large increase in κ between 0.65 and 0.85 GPa during pressurization indicated the presence of a phase transformation into the high-pressure phase at a pressure slightly lower than observed at 290 K. However, on decreasing pressure the reverse transformation did not start until below 0.15 GPa, showing a significant increase in the transition hysteresis. To avoid breaking the probe wire we did not go below 0.1 GPa, and the transformation was completed only during re-heating at 0.1 GPa. Unfortunately, in spite of this careful treatment the wire broke on heating near room temperature.

The temperature dependence of κ in a well-ordered phase is expected to be $\kappa \sim T^{-1}$, whereas disordered states such as glasses show a much weaker dependence such that κ is typically almost independent of temperature at these relatively high temperatures. Consequently, the temperature dependence gives a rough indication concerning the degree of order of the phases. The thermal conductivity of the low pressure phase varies as $\kappa \sim T^{-1.1}$, and in the high-pressure phase as $\kappa \sim T^{-1.2}$. Thus, we can conclude that both the low pressure and the high-pressure phases are well-ordered in terms of their $\kappa(T)$. The large difference in k between the phases must be connected with the structural change, but it cannot be easily associated with any of the suggested structures. In terms of simple theory for κ of a crystal with monoatomic basis [22], the large increase indicates a large increase of the Debye temperature, i.e. the elastic constants, and/or a significant reduction of the lattice anharmonicity.

3.4. Differential thermal analysis and the phase diagram

After the failure of the hot-wire probe, further data about the phase boundaries were collected by DTA in the same experiment. As shown in Fig. 8b, DTA measurements were in excellent agreement with the thermal conductivity measurements regarding the transformation coordinates. The centres of the exo- and endothermal peaks observed by DTA are observed at almost exactly the pressures where the thermal conductivity is half-way between the values observed for the pure phases. Since the transition line for the transformation into the high-pressure phase was rather well defined by the points already obtained, we concentrated on finding the transition line for the transformation back to the ambient-pressure phase. We therefore completed two further pressure-temperature cycles, in both cases increasing pressure through the transformation up to 1 GPa near 270 K, cooling in the high-pressure state to a suitable temperature, then decreasing pressure and allowing the vessel to warm up to near room temperature at pressures of 0.1 and 0.2 GPa, respectively. In both cycles we were able to observe the reverse transformation during the isobaric low-pressure heating part of the cycle, with transition temperatures in very good agreement with those obtained in the thermal conductivity experiments.

Finally, we tried to verify the intermediate-temperature part of the phase diagram, as mapped by Pistorius [11]. We made an isobaric run at 0.2 GPa to 400 K to find the transition into the high-temperature low-pressure phase, but during a subsequent isothermal pressure run to 1.1 GPa and back at 403 K, crossing several phase boundaries, one of the thermocouples broke and the experiment was terminated.

The experimental results discussed in Sections 3.3 and 3.4 were used to plot the low-temperature phase diagram of $LiBH_4$ in Fig. 9. The full lines drawn in the high-temperature part of the diagram have been re-plotted from Fig. 2 of Pistorius [11]. Our data for the transition

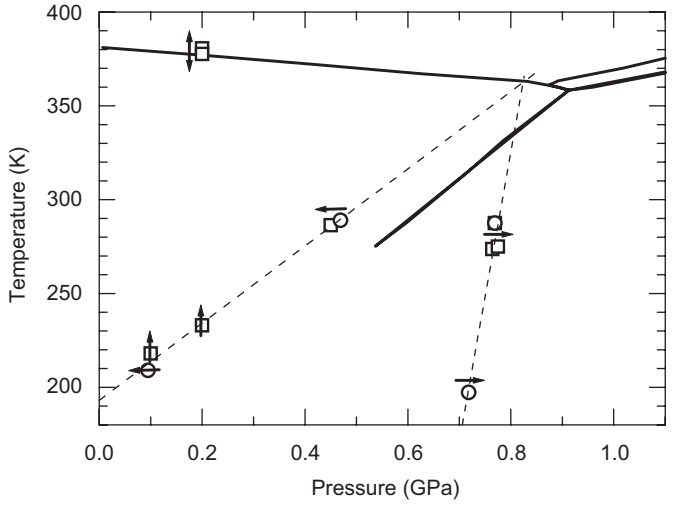

Fig. 9. Phase diagram for $LiBH_4$. Circles and squares show transition coordinates observed in thermal conductivity and DTA data, respectively. Arrows show direction of $P-T$ change in experiments. Full lines correspond to phase boundaries in the $P-T$ diagram given by Pistorius [11], dashed lines the observed transition lines for transformations between the α and β phases in this work (see text for details).

coordinates are plotted as squares and circles. We have defined these coordinates as the coordinates for the maxima (or minima) in the DTA signals, or for the halfway points observed for the transitions in the data for κ. As noted above, there is a very strong hysteresis in the transition pressure, and the hysteresis increases rapidly with decreasing temperature. However, both branches of the transformation line have positive slopes dT/dp; since the transition is exothermic on pressure increase (Fig. 8b), the slope of the phase line must be positive. Linear extrapolation shows that the hysteresis should be zero and the transition exactly reversible at about 358 K and 0.81 GPa. We conclude that this point corresponds to the triple point identified by Pistorius at the same temperature but about 0.1 GPa higher in pressure. This pressure difference may be due to sample properties, such as a different sample purity, but might also in part be due to the friction correction for decreasing pressures mentioned in the last section. Since this friction correction is usually proportional to the load applied, an increased correction should push the observed triple point toward higher pressures and lower temperatures. The data suggest that the transformation $\alpha \rightarrow \beta$ can never occur at atmospheric pressure, in agreement with the fact that no such transformation has been reported; even at absolute zero the transformation from the low-pressure phase into the β phase should not occur below 0.6 GPa. Conversely, once the β phase has formed it is very stable and even at atmospheric pressure the reverse transformation back to the α phase does not occur until the temperature has been raised to above 190 K. We have not been able to measure the equilibrium phase line. Defining this, to a first approximation, as the average of the two transition lines valid for the respective directions we find that the equilibrium temperature at atmospheric pressure is close to 55 K. The large average slope dT/dp ($\sim$370 K GPa^{-1}) deduced from this value indicates that the entropy difference is small between the two phases, and the large hysteresis suggests that there is a significant energy threshold for the transformation.

4. Conclusions

The phase transition from the ambient pressure α-$LiBH_4$ phase into the room-temperature high-pressure modification (β-$LiBH_4$) was observed by Raman spectroscopy and XRD. The structure of the high-pressure phase could not be identified but is different from those theoretically predicted [16,17]. The low-temperature phase diagram up to 370 K was mapped in detail for the first time using thermal conductivity and DTA measurements. The results show that although the β phase is metastable at atmospheric pressure below about 200 K, no transition into this phase can occur at pressures below about 600 MPa. The previously reported phase transition [11] near 380 K at atmospheric pressure was also confirmed.

Acknowledgments

This work was financially supported by Carl Tryggers Stiftelse för Vetenskaplig Forskning, Magn. Bergvalls Stiftelse, DAAD, and DFG. High-pressure experiments with XRD were performed at the Bayerisches Geoinstitut under the EU "Research Infrastructures: Transnational Access Programme (Contract No. 505320 (RITA)-High Pressure).

References

[1] P. Vajeeston, P. Ravindran, R. Vidya, H. Fjellvåg, A. Kjekshus, Appl. Phys. Lett. 82 (2003) 2257.
[2] P. Vajeeston, P. Ravindran, R. Vidya, H. Fjellvåg, A. Kjekshus, Phys. Rev. B 68 (2003) 212101.
[3] A.V. Talyzin, B. Sundqvist, Phys. Rev. B 70 (2004) 180101.
[4] A.V. Talyzin, B. Sundqvist, High Pressure Res. 26 (2006) 165.
[5] C. Moysés Araújo, R. Ahuja, A.V. Talyzin, B. Sundqvist, Phys. Rev. B 72 (2005) 054125.
[6] R.S. Kumar, A.L. Cornelius, Appl. Phys. Lett. 87 (2005) 261916.
[7] B. Sundqvist, O. Andersson, Phys. Rev. B 73 (2006) 092102.
[8] J-Ph. Soulié, G. Renaudin, R. Černý, K. Yvon, J. Alloys Compds. 346 (2002) 200.
[9] K.N. Semenenko, A.P. Chavgun, V.N. Surov, Russ. J. Inorg. Chem. 16 (1971) 271.
[10] S. Orimo, Y. Nakamori, A. Züttel, Mater. Sci. Eng. B 108 (2004) 51.
[11] C.W.F.T. Pistorius, Z. Phys. Chem. N. Folge 88 (1974) 253.
[12] A. Züttel, S. Rentsch, P. Fischer, P. Wenger, P. Sudan, Ph. Mauron, Ch. Emmenegger, J. Alloys Compds. 356 (2003) 515.
[13] H.C. Johnston, N.C. Hallet, J. Am. Chem. Soc. 75 (1953) 1467.
[14] C.C. Stephenson, D.W. Rice, W.H. Stockmayer, J. Chem. Phys. 21 (1953) 1311.
[15] N.C. Hallet, H.L. Johnston, J. Am. Chem. Soc. 75 (1953) 1496.
[16] Z. Łodziana, T. Vegge, Phys. Rev. Lett. 93 (2004) 145501.

[17] P. Vajeeston, P. Ravindran, A. Kjekshus, H. Fjellvåg, J. Alloys Compds. 387 (2005) 97.
[18] T.J. Frankcombe, G.-J. Kroes, A. Züttel, Chem. Phys. Lett. 405 (2005) 73.
[19] B. Håkansson, P. Andersson, G. Bäckström, Rev. Sci. Instrum. 59 (1988) 2269.
[20] S. Gomes, H. Hagemann, K. Yvon, J. Alloys Compds. 346 (2002) 206.
[21] S. Orimo, Y. Nakamori, G. Kitahara, K. Miwa, N. Ohba, S. Towata, A. Züttel, J. Alloys Compds. 404–406 (2005) 427.
[22] R.G. Ross, P. Andersson, B. Sundqvist, G. Bäckström, Rep. Prog. Phys. 47 (1984) 1347.